NUREG/CR-6875
ANL-04/08

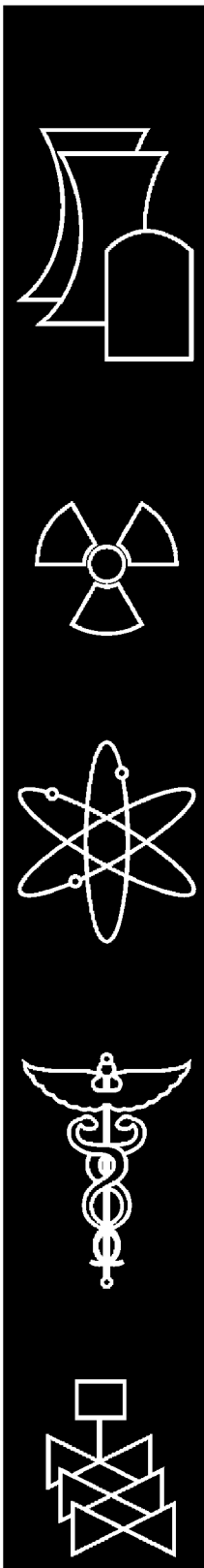

Boric Acid Corrosion of Light Water Reactor Pressure Vessel Materials

Argonne National Laboratory

U.S. Nuclear Regulatory Commission
Office of Nuclear Regulatory Research
Washington, DC 20555-0001

NUREG/CR-6875
ANL-04/08

Boric Acid Corrosion of Light Water Reactor Pressure Vessel Materials

Manuscript Completed: May 2004
Date Published: July 2005

Prepared by
J.-H. Park, O. K. Chopra, K. Natesan, and W. J. Shack

Energy Technology Division
Argonne National Laboratory
9700 South Cass Avenue
Argonne, IL 60439

W. H. Cullen, Jr., NRC Project Manager

Prepared for
Division of Engineering Technology
Office of Nuclear Regulatory Research
U.S. Nuclear Regulatory Commission
Washington, DC 20555-0001
NRC Job Code Y6722

Abstract

This report presents experimental data on electrochemical potential and corrosion rates of the materials found in the reactor pressure vessel head and control rod drive mechanism (CRDM) nozzles in boric acid solutions of varying concentrations at temperatures of 95–316°C (203–600°F). Tests were conducted in (a) high–temperature, high–pressure aqueous solutions with a range of boric acid concentrations, (b) high-temperature (150–316°C) H-B-O solutions at ambient pressure, wetted and dry, and (c) low–temperature (≈95°C) saturated, aqueous, boric acid solutions. These correspond to the following situations: (a) low leakage through the nozzle and nozzle/head annulus plugged, (b) low leakage through the nozzle and nozzle/head annulus open, and (c) significant cooling due to high leakage and nozzle/head annulus open. The results indicate significant corrosion only for the low–alloy steel and no corrosion for Alloy 600 or 308 stainless steel cladding. Also, corrosion rates were significant in saturated boric acid solutions, and no material loss was observed in boric acid melts or deposits in the absence of moisture. The results are compared with the existing corrosion/wastage data in the literature.

Foreword

In the aftermath of the discovery of a corrosion cavity in the vessel head at the Davis-Besse Nuclear Power Station in March 2002, the U.S. Nuclear Regulatory Commission (NRC) renewed its effort to understand the mechanics and chemistry that occur during the corrosion process. Based on the results of corrosion testing over the preceding 15 or so years, the prevailing thinking at that time was that corrosion in an aqueous-based solution could not occur at an elevated temperature, because water would evaporate and dry boric acid salts were "known" to be non-corrosive. However, such thinking did not account for the corrosion rates that had prevailed on the Davis-Besse reactor head. Against that background, the NRC's Office of Nuclear Regulatory Research, together with Argonne National Laboratory, completed a test program to determine the corrosion rates of important reactor structural materials over a wide range of temperatures and boric acid solution concentrations. This report presents the resultant corrosion rate and electrochemical potential data.

As part of the investigation of the Davis-Besse reactor head corrosion event, industry analysts developed a model that suggested that the evaporative cooling effect would reduce the temperature of the pool of accumulating liquid to about 93 °C (200 °F) as the leak rate approached and exceeded about 0.4 liter (0.1 gallon) per minute. This finding is important because this temperature is significantly cooler than assumed in earlier testing and does not support the thinking that an aqueous-based boric acid solution would not exist because the water would evaporate. This report contains data showing that corrosion rates of low-alloy steel at that temperature are a strong function of solution concentration, and reach about 100 mm (3.9 inches) per year in saturated solutions. Further, this report describes, for the first time, tests in slightly wetted boric acid salts at temperatures of 150 °C (302 °F) and 170 °C (338 °F). The data from these tests show that corrosion rates of low-alloy steel in this mixture can actually exceed those of aqueous solutions, reaching 125 mm (4.9 inches) to 150 mm (5.9 inches) per year at 150 °C (302 °F).

On a positive note, this report contains data showing that stainless steel cladding materials and Alloy 600 do not corrode significantly in any combination of temperature and solution concentration tested within the scope of this program. Likewise, the electrochemical potential (ECP) values for the materials and solutions tested in this program support the conclusion that ECP differences among the relevant combinations of structural materials are too small to give rise to the possibility of any significant galvanic reactions.

The data derived from this study will expand the existing database of corrosion rates for reactor structural materials in boric acid solutions, and much of the data will be included in the Boric Acid Corrosion Guidebook (Reference 5). Nonetheless, when applying any conclusions based on these data, users should remain within the bounds of the tested parameters; extrapolation of these results could lead to erroneous conclusions. Users should also be aware that composition differences among reactor and low-carbon steels could result in inaccurate estimates of corrosion rates for materials that were not actually tested in this program.

Carl J. Paperiello, Director
Office of Nuclear Regulatory Research
U.S. Nuclear Regulatory Commission

Contents

Abstract iii

Foreword v

Contents vii

Executive Summary xiii

Abbreviations xv

Acknowledgments xvii

1. Introduction 1

2. Experimental 7

2.1 Materials 7

2.2 Test Environments 8

2.2.1 Low–Temperature Saturated Boric Acid Solutions 8

2.2.2 High–Temperature High–Pressure PWR Environments 10

2.2.3 Molten H–B–O Environments at Ambient Temperature 11

2.3 Test Facilities 12

2.3.1 Low–Temperature Tests at Ambient Pressure 12

2.3.2 High–Temperature High–Pressure Tests 14

2.3.3 Tests in Molten H–B–O Environment at Ambient Pressure 16

2.3.4 Capsule Test 20

3. Results 21

3.1 ECP and Potentiodynamic Measurements 21

3.1.1 Low–Temperature Tests at Ambient Pressure 21

3.1.2 Tests in Molten H–B–O System at Ambient Pressure 23

3.1.3 Tests in High–Temperature High–Pressure Aqueous Solutions 24

3.2 Wastage Corrosion Tests 25

3.2.1 Saturated Boric Acid Solution at 97.5°C 25

3.2.2 Molten H–B–O Environment at Ambient Pressure 30

3.2.3 High–Temperature High–Pressure Boric Acid Solutions 32

3.2.4 Effect of Chromium Content on Corrosion Rate 36

4. Discussion 39

5. Summary 45

References 47

Figures

1. Reactor pressure vessel head at the Davis-Besse nuclear generating station 1

2. Severe corrosion on the exterior surface of the RPV head between CRDM nozzle #3 and nozzle #11 at the Davis-Besse nuclear power station 2

3. Schematic of the Davis–Besse CRDM nozzle showing the SS flange, Alloy 600 penetration, and J–groove weld between the RPV head and the penetration 3

4. Deposits of boric acid crystals on reactor pressure vessel head from leaking CRDM nozzles 3

5. Schematic drawing of the Type 308 SS weld overlay on A533 Gr.-B low-alloy steel.... 7

6. Ring samples fabricated from the Type 308 SMA weld overlay 8

7. Assembled set of ring samples of A533 Gr.-B low-alloy steel and Type 308 SS SMA weld overlay for corrosion/wastage tests 8

8. Solubility of boric acid in water vs. temperature..... 9

9. Plots of pH_T vs. temperature in the oxygen and argon gas environments for the RT–saturated solution and the boric acid saturated at T; pH_T vs. wppm B for temperature between RT and 100°C; and pH_T and wppm B vs. inverse temperature. 10

10. Plot of equilibrium water vapor pressure vs. temperature for the H-B-O system 11

11. Electrochemical cell for potentiodynamic studies 12

12. Schematic drawing of the working electrode 12

13. Calibration of the potentiodynamic test apparatus following with ASTM G5-94 using Fe working electrode and saturated calomel reference electrode..... 13

14. Apparatus for corrosion test in concentrated solutions of boric acid at temperatures up to 100°C 13

15. Schematic of the facility for high–temperature high–pressure tests in PWR environments with various concentrations of B and Li 14

16. Schematic of the test chamber showing the location of various electrodes, solution inlet/outlet lines, and thermocouple well 15

17. A four hole high–purity alumina rod containing four working electrodes..... 15

18. Schematic of the test specimen holder for high-temperature, high-pressure corrosion tests in a flowing boric acid solution under the hydrogen cover gas..... 16

19. Schematic of the facility for potentiodynamic and ECP measurements in mixtures of molten boric acid and boric oxide at temperatures up to 300°C 16

20. Change in weight of boric acid when heated from 25 to 450°C in an air environment, corresponds to transition to HBO_2 and represents melting point of HBO_2 17

21. Weight change vs. time at 280°C in air atmosphere. Boric acid turns to HBO_2 and mostly B_2O_3 phase 17

22. A533 Gr.–B low–alloy steel working electrode 18

23. Reference electrode consisting of Ag/AgI electrolyte contained in a porous sintered ZrO_2 cup 18

24. The apparatus for conducting corrosion tests in molten H-B-O system with water additions 19

25. Photograph of the solid boric acid crust left at the bottom of the test chamber after the corrosion test with water addition 20

26. Test capsules 12.7 mm in diameter and 50 mm long, loaded with a boric acid solution saturated at room temperature and tested at 172, 235, 294, and 316°C 20

27. Typical plot of measured ECP vs. time for the A533 Gr.-B, Alloy 600, and 308 SS in saturated boric acid solution at ≈95°C and ambient pressure 21

28. Potentiodynamic test results for Type 304 stainless steel in aerated saturated solution of boric acid at ≈100°C 22

29. Potentiodynamic test results for A533 Gr.–B steel in an aerated saturated boric acid solution at 95°C 22

30. Photomicrograph of A533 Gr.–B low–alloy steel tested in deaerated boric acid solution containing 3500 wppm B at 95°C 23

31. Potentiodynamic test on A533 Gr.–B steel in molten H-B-O system at 290°C 23

32. Potentiodynamic test on A533 Gr.–B steel in molten HBO_2 + B_2O_3 system with addition of water 24

33. Change in ECP of A533 Gr.–B steel, Alloy 600, and 308 SS weld metal in water containing 1,000 or 9,090 ppm B, 2 ppm Li, and ≈2 ppm dissolved hydrogen at temperatures between 150 and 316°C and 12.4 MPa pressure 25

34. Ring-test specimen holder after 100-h exposure in aerated saturated boric acid solution at 97.5°C and after rinsing in ultra high–purity water 27

35. Ring-test specimen holder after 411–h exposure to aerated saturated boric acid solution at 97.5°C 27

36. A533 Gr.–B specimens exposed to aerated saturated boric acid solution at 97.5°C for times up to 411 h 27

37. Average corrosion rates for A533 Gr.–B in various boric acid solutions at 97.5°C 28

38. Geometry and metallographic evaluation of A533–Gr. B ring specimen exposed to deaerated saturated boric acid solution at 97.5°C for 411 h 29

39. Schematic representation for the corrosion of low–alloy steel investigated in the concentrated boric acid solutions 30

40. Corrosion specimens tested in H-B-O system at 170°C and ambient pressure 31

41. Measured corrosion rates for A533 Gr.–B steel in molten H–B–O system with additions of water 32

42. Measured corrosion rates for A533 Gr.–B steel at high temperature and pressure in a room-temperature saturated boric acid solution under hydrogen cover gas 32

43. Blossom–like deposits of iron borate on A533 Gr.–B sample exposed at 172°C and Fe_3O_4 deposits on the sample exposed at 294°C in room–temperature saturated boric acid solution inside a sealed capsule 34

44. Measured corrosion rates for A533 Gr.–B steel in various boric acid solutions 35

45. Electrical conductivity of pure water and B containing solutions 36

46. Effect of Cr concentration on the average corrosion rate in room-temperature-saturated boric acid solution at 150, 288, and 316°C and 12.4 MPa under H_2 cover gas 38

47. Measured corrosion rates for low–alloy steels in various solutions of boric acid at 80–104°C and ambient pressure 42

48. Measured corrosion rates for low–alloy steels in various solutions of boric acid at 80–170°C and ambient pressure 43

49. Measured corrosion rates for carbon and low–alloy steels in boric acid solutions at 12.4 MPa pressure 43

Tables

1. Composition of RPV head and nozzle alloys for corrosion studies 7

2. Melting points and phase transition temperatures in the H-B-O system 11

3. The ECP of A533 Gr.–B, Type 304 SS, 308 SS weld metal, and Alloy 600 in boric acid solutions at 95°C and ambient pressure 21

4. Measured ECP of various alloys in water containing 9,090 ppm B, 2 ppm Li, and ≈2 ppm dissolved hydrogen at temperatures between 25 and 316°C and 12.4 MPa pressure 24

5. Measured ECP of various alloys in water containing 1,000 ppm B, 2 ppm Li, and ≈2 ppm dissolved hydrogen at temperatures between 150 and 316°C and 12.4 MPa pressure 25

6. Average corrosion rates for A533 Gr.–B low-alloy steel in aerated and deaerated saturated solutions of boric acid at 97.5°C 26

7. Average corrosion rates for A533 Gr.–B low-alloy steel in aerated saturated and half-saturated solutions of boric acid at 97.5°C 26

8. Corrosion test results in dry H–B–O environment at 300, 260, and 150°C 30

9. Test results in H–B–O system at different temperatures 31

10. Weight change data for A533-Gr. B tested at high temperature and pressure in a room-temperature-saturated boric acid solution under hydrogen cover gas 33

11. Weight and change in wt.% vs. temperature for the samples exposed to room-temperature saturated boric acid solution in the capsule tests for 68 h 34

12. Compositions of the alloys exposed in room-temperature-saturated boric acid solution 37

13. Weight change data for the alloys tested at high temperature and pressure in a room-temperature-saturated boric acid solution under hydrogen cover gas 37

Executive Summary

In March 2002, during inspections at the Davis-Besse (D-B) nuclear power station in response to NRC Bulletin 2001-01, axial cracks were identified in five control rod drive mechanism (CRDM) nozzles near the J–groove weld. Also, significant degradation of the reactor pressure vessel (RPV) head base metal was discovered downhill of nozzle #3; a triangular cavity, ≈127 mm (5 in.) width and 178 mm (7 in.) long and completely through the low-alloy steel RPV head thickness (≈178 mm), had been created. Although cracking of Alloy 600 CRDM nozzles by primary water stress corrosion cracking (PWSCC) is a known degradation mechanism and has been observed at other nuclear power plants, damage of this magnitude to the RPV head caused by boric acid corrosion had not been anticipated. In the other instances of CRDM nozzle cracking, total leakage from the crack into the annulus appears to have been very low and occurred at very low leakage rates. At low leak rates (≈10^{-6} to 10^{-5} gpm), the leaking flow completely vaporizes to steam immediately downstream from the principal flashing location resulting in a dry annulus and no loss of material. The D-B experience demonstrates that this is not always the case.

It is important to understand the conditions that can result in this aggressive attack. The critical issue is why the leaking nozzle #3 at D-B progressed to high leak rates and significant RPV head wastage. Corrosion/wastage of RPV steel in concentrated boric acid solutions is not well described or quantified in the literature, and especially not under the temperature, flow, and concentration of species that may have occurred on the D-B head. The electrochemical potentials (ECPs) of the alloys in the aqueous solutions involved are also not known.

This report presents experimental data on ECP and corrosion/wastage rates of the materials found in the RPV head and nozzles of the D–B reactor in boric acid solutions of varying concentrations at temperatures of 95–316°C (203–600°F). Tests were conducted in environmental conditions that have been postulated in the CRDM nozzle/head crevice: (i) high–temperature, high–pressure aqueous environment with a range of boric acid solution concentrations; (ii) high-temperature (150–300°C) boric acid powder at atmospheric pressure with and without the addition of water; and (iii) low–temperature (≈95°C) saturated boric acid solution both deaerated and aerated. These environmental conditions correspond to the following situations: (a) low leakage through nozzle crack and nozzle/head annulus plugged, (b) low leakage through nozzle crack and nozzle/head annulus open, and (c) significant cooling due to high leakage through nozzle crack and nozzle/head annulus open.

Test facilities were assembled to perform ECP and corrosion rate measurements on A533 Gr.–B low–alloy steel, Alloy 600, and 308 SS weld clad, in the various postulated environments in the CRDM nozzle/head crevice. In general, the ECP of all alloys decreased with an increase in temperature. At temperatures below 150°C the ECP of A533 Gr.–B low–alloy steel was significantly lower than that of the other alloys. Also, at 95°C, the ECP of A533 Gr.–B steel decreased slightly as the concentration of boric acid in the solution was decreased from 36,000 ppm to 3,500 ppm. At 150–316°C and 12.4 MPa (1800 psi) pressure, the ECP of all alloys are comparable in water with 1000 or 9090 ppm B, ≈2 ppm Li, <10 ppb dissolved oxygen (DO), and ≈2 ppm dissolved hydrogen.

In the various environments investigated in the present study, the corrosion rates of Alloy 600 and 308 SS cladding were found to be negligible compared to those of A533 Gr.–B

steel. Also, in the absence of moisture, no corrosion was observed for any of the materials in H–B–O environments at 150, 260, and 300°C; the H–B–O environments consist of a dry powder of HBO_2 + H_3BO_3 at 150°C, molten HBO_2 at 260°C, and molten mixture of HBO_2 + B_2O_3 at 300°C.

For A533 Gr.–B steel, an average corrosion rate of ≈40 mm/y (1.6 in./y) was measured in aerated saturated solution of boric acid at 97.5°C and ambient pressure. The corrosion rate in aerated half–saturated solution was a factor of ≈2 lower than in saturated solution; the rates for deaerated solution were ≈40% lower than in aerated solution. Very high corrosion rates were observed for A533 Gr.–B steel at 140–170°C in molten salt solutions of boric acid with addition of water. Corrosion rates up to 150 mm/y were measured at 150°C.

The corrosion experiments in high–temperature high–pressure water containing 9090 ppm B, ≈2 ppm Li, <10 ppb DO, and ≈2 ppm dissolved hydrogen showed that the corrosion rates decreased with increasing temperature. The rates were ≈5 mm/y at 100–150°C and decreased to <0.1 mm/y at 316°C.

The existing corrosion/wastage data in the literature have been summarized. The results from the present study have been compared with the available data to assess the corrosion performance of the RPV and CRDM nozzle materials in boric acid solutions.

Abbreviations

ANL	Argonne National Laboratory
ASTM	American Society for Testing and Materials
BNL	Brookhaven National Laboratory
CGR	Crack growth rate
CR	Corrosion rate
CRDM	Control rod drive mechanism
D-B	Davis Besse
DO	Dissolved oxygen
ECP	Electrochemical potential
EDX	Energy dispersive x–ray spectroscopy
EPRI	Electric Power Research Institute
ID	Inner diameter
NDE	nondestructive examination
NRC	Nuclear Regulatory Commission
OD	Outer diameter
PWR	Pressurized water reactor
PWSCC	Primary water stress corrosion cracking
RCS	Reactor coolant system
RPV	Reactor pressure vessel
RT	Room temperature
SCE	Saturated calomel electrode
SEM	Scanning electron microscopy
SHE	Standard hydrogen electrode

SMA	Shielded metal arc
SS	Stainless steel
TGA	Thermogravimetric analysis
UHP	Ultra high purity
WE	Working electrode
wppm	parts per million by weight

Acknowledgments

The authors thank R. W. Clark and E. J. Listwan for their contributions to the experimental effort. This work is sponsored by the Office of Nuclear Regulatory Research, U.S. Nuclear Regulatory Commission, Job Code Y6722; Program Manager: W. H. Cullen, Jr.